U.S. National Library of Medicine
National Center for Biotechnology Information

NLM Citation: Zhang H. Ethyl-3,5-bis(acetylamino)-2,4,6-triiodobenzoate nanoparticles. 2008 Jun 10 [Updated 2008 Jul 30]. In: Molecular Imaging and Contrast Agent Database (MICAD) [Internet]. Bethesda (MD): National Center for Biotechnology Information (US); 2004-2013.
Bookshelf URL: https://www.ncbi.nlm.nih.gov/books/

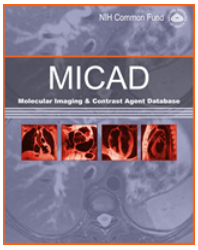

Ethyl-3,5-bis(acetylamino)-2,4,6-triiodobenzoate nanoparticles

N1177

Huiming Zhang, PhD[1]

Created: June 10, 2008; Updated: July 30, 2008.

Chemical name:	Ethyl-3,5-bis(acetylamino)-2,4,6-triiodobenzoate nanoparticles	
Abbreviated name:	N1177	
Synonym:		
Agent Category:	Triiodobenzoate	
Target:	Macrophages	
Target Category:	Phagocytosis	
Method of detection:	X-ray computed tomography (CT)	
Source of signal/contrast:	Iodine	
Activation:	No	
Studies:	• *In vitro* • Non-primate non-rodent mammals	No structure is currently available in PubChem.

Background

[PubMed]

Macrophages are key cellular mediators of inflammation in atheroma and participate in all stages in evolving atherosclerotic plaques (1, 2). The atheroma lesion is normally initialized by recruiting monocytes in inflamed intima. Monocytes mature into macrophages under the *in situ* stimulation of overexpressed macrophage colony-stimulating factor. As cholesteryl esters gradually accumulate in cytoplasm, macrophages are converted into foam cells at the early stage of atheroma. The accumulation of foam cells leads to the formation of fatty streaks and the deposition of fibrous tissues, which indicates the progression of atheroma into an intermediate stage. Fibrous caps are formed on the surface of a lipid-rich core and result in vulnerable atherosclerotic plaque as the smooth muscle cells synthesize bulk extracellular matrix. Finally, the rupture of the atherosclerotic plaques and the calcification of vessel walls progressively occlude the lumen. The vulnerable plaques are considered as a "high-risk" stage, which contain much higher levels of macrophages than that in any other stage (3). Thus, measuring macrophage density in plaques becomes an alternative approach to evaluate the vulnerable plaques

Author Affiliation: 1 National Center for Biotechnology Information, NLM, NIH, Bethesda, MD; Email: micad@ncbi.nlm.nih.gov.

(4). Atherosclerotic plaques can be generated in rabbits by balloon injury in the aortas followed by hypercholesterolemic diet (4). This animal model provides high levels of macrophages with sizes similar to those found in the human coronary atherosclerotic plaques, suitable for examining the effects of antiatherosclerotic drugs on atherosclerotic plaque size and composition.

Multi-detector row computed tomography (MDCT) has been used as a robust imaging modality for non-invasive assessment of coronary arteries (5, 6). In particular, the development of 64-slice MDCT (64-MDCT) provides fast gantry rotation time (0.33 s) and small imaging voxel size (0.4 mm^3) (7), which allows for reliable assessment of atherosclerotic plaques (8). Because their CT attenuation differences are much larger than 30 HU (a criteria in delineation of tissues), calcified plaques (391–419 HU), fibrous plaques (70–104 HU), and lipid-rich plaques (soft plaques, 14–49 HU) can be directly differentiated with the use of MDCT (8). To measure the macrophage density in the plaques requires a macrophage-specified CT contrast agent (4). Iodinated compounds have been used as CT contrast agents for many years. Small molecules such as iopamidol can attenuate the X-ray density up to 30 HU at a dosage of 1 mg iodine/g tissue (9), but they are not specific imaging agents for macrophages. Contrast agents can be incorporated into macrophages through phagocytosis, a special macrophage uptake process. Sparingly soluble crystals, supramolecular aggregates, large micelles, or emulsions of iodinated lipids are suitable for this purpose. All of these contrast agents should have a sufficiently large size to be marked ("opsonized") by circulating proteins ("opsonins"), then followed by phagocytosis (9). Ethyl-3,5-bis(acetylamino)-2,4,6-triiodobenzoate nanoparticles (N1177) is an emulsified suspension that is composed of crystalline iodinated particles dispersed with surfactant (4). The iodinated particles, ethyl-3,5-bis(acetylamino)-2,4,6-triiodobenzoate, are an esterified derivative of the X-ray contrast agent diatrizoic acid with a very low aqueous solubility (~2 μg/ml). Two biocompatible surfactants, a polyoxyethylene-polyoxypropylene block co-polymer (poloxamer 338) and a polyethylene glycol, are added to stabilize the particles and prevent aggregation.

Synthesis

[PubMed]

Hyafil et al. reported the detailed synthesis of N1177 (4). Initially, 6-ethoxy-6-oxohexy-3,4-bis(acetylamino)-2,4-triiodobenzoate ($C_{19}H_{23}I_3N_2O_6$), also called iodinated aroyloxy ester, was obtained by condensation of 6-bromohexanoate with sodium diatrizoate in dimethyl formamide followed by precipitation in dimethyl sulfoxide. The produced iodinated aroyloxy ester was milled with poloxamer 338 in the presence of inert beads to generate a nanoparticulate suspension, which was separated from the beads by membrane filtration with membrane pore diameter of 2–5 μm. Then, polyethylene glycol 1450 and tromethamine were added to the obtained suspension to stabilize the particles and to maintain a neutral pH. The final product (N1177) was composed of 150 mg/ml of iodinated aroyloxy ester, 30 mg/ml of poloxamer 338, 150 mg/ml of polyethylene glycol 1450, and 0.36 mg of tromethamine, and remained stable for ~8 months. The size of N1177 particle ranged from 153 nm to 408 nm with a mean value of 259 nm. Transmission electron microscopy of N1177 demonstrated that cores formed by electron-dense granules were covered by molecular polymers, and iodine was present in the electron-dense granules.

In Vitro Studies: Testing in Cells and Tissues

[PubMed]

Hyafil et al. examined the *in vitro* uptake of N1177 in mouse macrophages (4). After incubation with N1177 (n = 6 mice) or iopamidol (n = 6 mice) as control for 1 h, numerous dark granules were observed in the cytoplasm of macrophages that were incubated with N1177. The cell-internalized iodine was quantified with inductively coupled plasma mass spectrometry, which revealed a substantially higher uptake of N11777 by macrophages as compared to uptake by iopamidol (4,920 ± 1,019 *versus* 56 ± 11 μg iodine/g cell pellets).

Animal Studies

Rodents

[PubMed]

No publication is currently available.

Other Non-Primate Mammals

[PubMed]

The pharmacokinetics of N1177 was measured in healthy rabbits (4). After rabbits (n = 8) intravenous injections of N1177 at a dose of 250 mg iodine/kg, a series of CT images were collected to examine the enhancement in the blood and in macrophage-rich tissues. At 5 minutes after injection, the X-ray absorption value was found to be 125.3 ± 14.1 HU in the aortic lumen. This enhancement allowed for clear delineation of all major arterial and venous contours by CT. Two hours after injection of N1177, the vascular enhancement of N1177 was decreased rapidly, i.e., the absorption value measured in the aortic lumen returned to its precontrast level (42.3 ± 3.7 HU), whereas the enhancement in macrophage-rich tissues such as spleen and liver was significantly higher than that of precontrast level: 106.7 ± 6.5 *versus* 65.2 ± 2.2 HU in the spleen, and 114.4 ± 10.3 *versus* 63.1 ± 5.1 HU in the liver. No CT enhancement was found in other macrophage-deficient organs, such as muscles. A low enhancement in kidneys and in the urinary tract 1 h after injection of N1177 was caused by the renal excretion of N1177. No residual enhancement was detectable 24 h after the injection of N1177. As a control, the same rabbit was imaged 1 week later, followed by injection of iopamidol at 250 mg iodine/kg. The X-ray absorption value was much lower, 61.8 ± 13.9 HU at 5 min after injection of iopamidol. No enhancement was found in spleen and liver 2 h later.

The *in vivo* uptake of N1177 in macrophages was examined in atherosclerotic plaques in rabbits (n = 8) (4). The atherosclerotic plaques were generated by double balloon injuries in the aortas within one month's time, followed by 4 months of hypercholesterolemic diet. Healthy rabbits (n = 4) with a chow diet were used as control. All rabbits were first imaged with 64-MDCT after injection of iopamidol, and they were imaged again 1 week later after injection of N1177 at a dose of 250 mg iodine/kg. All CT images were collected at 2 h after injection, when enhancement of macrophage-rich tissues reached the highest value and the enhancement in the aortic lumen decreased to nearly zero, which allowed for clear discrimination between the macrophage-rich atherosclerotic plaques and the aortic lumen in the images. The enhancement in atherosclerotic plaques was 13.3 ± 1.0 HU for N1177 and 4.1 ± 0.9 HU for iopamidol. For the control rabbits, no substantial enhancement was found in the arterial wall at 2 h after injection of N1177 (0.9 ± 1.2 HU) or iopamidol (0.3 ± 1.3 HU). After the imaging experiment, the aortas were excised for histological analysis of fibrous caps and lipid-rich cores in the atherosclerotic plaques. The results exhibited a correlation between the enhancement of N1177 on the CT image at 2 h and the intensity of macrophage infiltration in the corresponding histological section. A CT contrast enhancement ≥13.3 HU corresponded to a macrophage area extending to >20% of the intimal area. No macrophage was found in the aortic wall of control rabbits. Transmission electron microscopy demonstrated the presence of a large number of electron-dense granules in the lysosomes of macrophages in the atherosclerotic plaques of the excised tissues. Energy dispersion spectrometry confirmed that these granules showed contained iodine caused by the accumulation of N1177 in macrophages of atherosclerotic plaques.

Non-Human Primates

[PubMed]

No publication is currently available.

Human Studies

[PubMed]

No publication is currently available.

NIH Support

HL 71021, HL 78667

References

1. Jaffer F.A., Libby P., Weissleder R. Molecular and cellular imaging of atherosclerosis: emerging applications. J Am Coll Cardiol. 2006;47(7):1328–38. PubMed PMID: 16580517.
2. Packard R.R., Libby P. Inflammation in atherosclerosis: from vascular biology to biomarker discovery and risk prediction. Clin Chem. 2008;54(1):24–38. PubMed PMID: 18160725.
3. Yan Z.Q., Hansson G.K. Innate immunity, macrophage activation, and atherosclerosis. Immunol Rev. 2007;219:187–203. PubMed PMID: 17850490.
4. Hyafil F., Cornily J.C., Feig J.E., Gordon R., Vucic E., Amirbekian V., Fisher E.A., Fuster V., Feldman L.J., Fayad Z.A. Noninvasive detection of macrophages using a nanoparticulate contrast agent for computed tomography. Nat Med. 2007;13(5):636–41. PubMed PMID: 17417649.
5. Schmid M., Pflederer T., Jang I.K., Ropers D., Sei K., Daniel W.G., Achenbach S. Relationship between degree of remodeling and CT attenuation of plaque in coronary atherosclerotic lesions: an in-vivo analysis by multi-detector computed tomography. Atherosclerosis. 2008;197(1):457–64. PubMed PMID: 17727859.
6. Schroeder S., Kopp A.F., Burgstahler C. Noninvasive plaque imaging using multislice detector spiral computed tomography. Semin Thromb Hemost. 2007;33(2):203–9. PubMed PMID: 17340470.
7. Flohr T.G., McCollough C.H., Bruder H., Petersilka M., Gruber K., Suss C., Grasruck M., Stierstorfer K., Krauss B., Raupach R., Primak A.N., Kuttner A., Achenbach S., Becker C., Kopp A., Ohnesorge B.M. First performance evaluation of a dual-source CT (DSCT) system. Eur Radiol. 2006;16(2):256–68. PubMed PMID: 16341833.
8. Pohle K., Achenbach S., Macneill B., Ropers D., Ferencik M., Moselewski F., Hoffmann U., Brady T.J., Jang I.K., Daniel W.G. Characterization of non-calcified coronary atherosclerotic plaque by multi-detector row CT: comparison to IVUS. Atherosclerosis. 2007;190(1):174–80. PubMed PMID: 16494883.
9. Krause W. Delivery of diagnostic agents in computed tomography. Adv Drug Deliv Rev. 1999;37(1-3):159–173. PubMed PMID: 10837733.